

Characterization of shrub distribution using high spatial resolution remote sensing: Ecosystem implications for a former Chihuahuan Desert grassland

Ian O. McGlynn^{*}, Gregory S. Okin¹

Department of Environmental Sciences, University of Virginia, Charlottesville, VA 22904-4123, United States

Received 10 October 2005; received in revised form 18 January 2006; accepted 28 January 2006

Abstract

Patchiness is often considered a defining quality of ecosystems in arid and semiarid regions. The spatial distribution of vegetation patches and soil nutrients coupled with wind and water erosion as well as biotic processes are believed to have an influence on land degradation. A geostatistical measure of spatial “connectivity” is presented to directly measure the size of patches in the landscape from a raster data set. Connectivity is defined as the probability that adjacent pixels belong to the same type of patch. Connectivity allows the size distribution of erodible patches to be quantified from a remote sensing image or field measurement, or specified for the purposes of modeling.

Applied to high-resolution remote sensing imagery in the Jornada del Muerto Basin in New Mexico, the spatial distribution of plants indicates the current state of grassland-to-shrubland transition in addition to processes of degradation in this former grassland. Shrub encroachment is clearly evident from decreased intershrub patch size in coppice dunes of 27.8 m relative to shrublands of 65.2 m and grassland spacing of 118.9 m. Shrub patches remain a consistent 2–4 m diameter regardless of the development of bush encroachment. A strong SW–NE duneland orientation correlates with the prevailing wind direction and suggests a strong aeolian control of surface geomorphology.

With appropriate data sets and classification, potential applications of the connectivity method extend beyond vegetation dynamics, including mineralogy mapping, preserve planning, habitat fragmentation, pore spacing in surface hydrology, and microbial community dynamics.

© 2006 Elsevier Inc. All rights reserved.

Keywords: Connectivity; Spatial distribution; Shrub encroachment; Aeolian geomorphology; Desert vegetation; Chihuahuan Desert; Mesquite

1. Introduction

Shrub encroachment is a global phenomenon documented in arid and semiarid regions of Africa, Australia, and North America (Archer, 1995; Fensham et al., 2005; Roques et al., 2001). In the Chihuahuan Desert grasslands of North America, shrub encroachment has been especially pronounced, with significant transformation of vegetation community structure occurring in the last 150 years. Populations of grasses, primarily black grama (*Bouteloua eriopoda*) once dominated 90% of the region but have diminished to less than 25% (Buffington & Herbel, 1965; Gibbens et al., 2005). Drought-resistant shrub cover, primarily comprised of creosote (*Larrea tridentata*) and

mesquite (*Prosopis glandulosa*), has increased by a factor of 10 over the same period, replacing the native grasses (Gibbens et al., 2005; Rango et al., 2000; Reynolds et al., 1999). Causes of shrub encroachment and grassland deterioration such as rainfall variability, elevated CO₂, changes in fire regime, seed dispersal and livestock grazing have been suggested (Archer et al., 1995; Scanlon et al., 2005), but the definitive cause of the transformation remains unknown (Archer, 1995; Bahre & Shelton, 1993; Dougill & Thomas, 2004).

The change in the spatial distribution of vegetation is an important aspect of shrub invasion. Shrubs create “islands of fertility” by trapping soil resources beneath their canopies (Schlesinger et al., 1990; Whitford, 1992). The transition from grass to shrub cover increases the scale of spatial heterogeneity and the dominant small-scale processes can be reflected through the position of individual plants (Schlesinger & Pilmanis, 1998). Thus, the ability to quantify the spatial distribution of plants could indicate the current state of

^{*} Corresponding author. Tel.: +1 434 924 6421; fax: +1 434 982 2137.

E-mail addresses: imcglynn@virginia.edu (I.O. McGlynn), okin@virginia.edu (G.S. Okin).

¹ Tel.: +1 434 924 3324; fax: +1 434 982 2137.

transition in addition to processes of degradation in semiarid mixed-shrub grasslands.

Remote sensing provides an opportunity to monitor and understand spatial patterns of vegetation and to inform the understanding of biotic and abiotic processes related to those patterns. The physical and spectral properties associated with vegetation cover and surface morphologic structures observed by remote sensing are being continuously refined (Bradley & Mustard, 2005; Okin & Painter, 2004; Okin et al., 2001; Weeks et al., 1996) especially with the incorporation of spatial patterns of vegetation (Caylor et al., 2004; Okin & Gillette, 2001; Privette et al., 2004; Scholes et al., 2004).

High spatial resolution remote sensing enables direct imaging of plant individuals that are at least the size of the ground resolution of the remote sensing image. This capability makes possible demographic studies of vegetation such as Schlesinger and Gremenopoulos's (1996) use of archival photographs to show that there were not climate-induced changes in woody vegetation in the Sudan from 1943 to 1994, and with individual-based monitoring of vegetation change in the Jornada Basin (Rango et al., 2002).

The ability to image individual plants with high resolution remote sensing opens up the possibility of effective use of geostatistical methods for describing the distribution of plants. Phinn et al. (1996) and Okin and Gillette (2001) have shown that traditional variograms can provide an accurate measure of average plant spacing in shrublands of the Chihuahuan Desert. Nonetheless, variograms provide limited information about the landscape. In particular, because variograms are calculated on the basis of pairs of data separated by some distance (lag), this method cannot provide information about conditions between these pairs. In landscapes where the connectedness of soil or vegetation patches (providing conduits for wind, water, seeds, small mammals, etc.) is important, a different geostatistical metric of two-dimensional landscape structure is advisable.

A new application of geostatistical techniques is presented to evaluate the connectivity of plant and soil patches. This connectivity function calculates the probability that contiguous pixels belong to the same class, or in this application, the probability that contiguous pixels are or are not occupied by shrubs.

In this study, we present the use of connectivity to provide spatial information about patch size and anisotropy and show that the results are robust for patchy landscapes. Using an object-oriented classification on digitized orthophotos of our field site in New Mexico, individual 1 m pixels are separated

into shrub and not-shrub classes. We then apply the connectivity statistic to the classified images to characterize the spatial nature of shrub encroachment and the spatial characterization of individual shrub patches. As a geostatistical measure, the use of connectivity is independent of the choice of classification scheme. The progressive nature of shrub encroachment is evaluated through the comparison of shrub and intershrub patch characteristics amongst differing areas of establishment. Specifically, we present the theory and definition of connectivity geostatistics, provide validation of connectivity based on stochastic simulation, and demonstrate the utility of connectivity using a case study to examine the variability of spatial distribution of vegetation in the Jornada Basin of New Mexico.

2. Material and experimental methods

2.1. Connectivity

We used a geostatistical measure of the connectedness of patches in the landscape called “connectivity.” For a raster data set, connectivity is defined as:

$$C(\vec{h}) = \frac{1}{n} \sum_n \left(\prod_{\vec{h}} I_i \right) \tag{1}$$

where C is the connectivity, \vec{h} is the lag vector with length $|h|$, n is the number of consecutive sets of pixels along \vec{h} in an image, and I_i is an indicator variable equal to 1 for pixels that belong to the class of interest and 0 otherwise. The connectivity at $\vec{h} = 0$ is denoted as C_0 and is equal to the fraction of pixels in an image that belong to the class of interest. For example, if “shrub” is the class of interest, then pixels that are classified as “shrub” are given a value of 1, and all other pixels are given a value of 0. In this case, C_0 will be equal to the fraction of pixels that are classified as “shrub”, or in other words, the fractional shrub cover.

Connectivity may also be interpreted as a probability. In the case of C_0 , the connectivity is the probability that any pixel in an image belongs to the class of interest. $C(\vec{h})$ is the probability that any set of consecutive pixels along \vec{h} all belong to the class of interest (Fig. 1). When interpreted as probabilities, it is intuitive that connectivity always decreases with increasing lag distance, $|h|$.

In practice, the decrease in connectivity with $|h|$ approximates an exponential decay function (Fig. 2). Thus, to derive a single statistic for the spatial scale of landscape connectedness

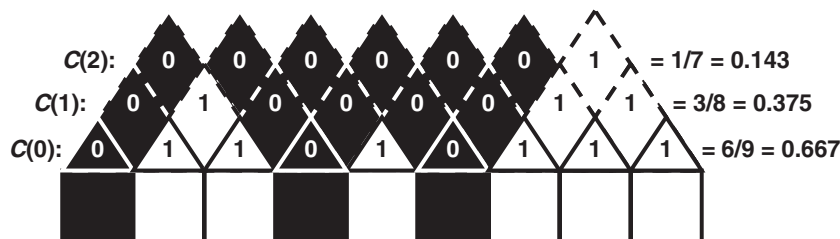


Fig. 1. Connectivity is calculated on the number of consecutive sets of pixels in an image, as 1 for pixels that belong to the class of interest and 0 otherwise with increasing lag distance, as demonstrated for 1, 2, and 3 pixel distances.

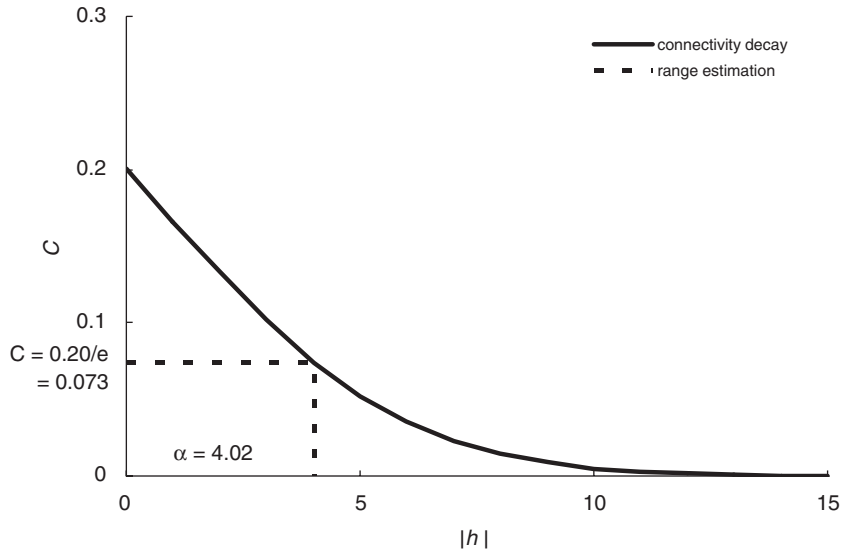


Fig. 2. Representative connectivity curve for 20% cover, a range of 4.02 (dashed line) and generally approximates an exponential decay curve.

similar to the “range” in traditional variograms, we modeled connectivity as:

$$C(\vec{h}) = C_0 \exp\left(-\frac{|\vec{h}|}{\alpha}\right) \quad (2)$$

From Eq. (2), it is clear that the range (α) is an e -folding distance at which the connectivity drops to C_0/e .

Lag is treated as a vector \vec{h} , allowing for connectivity to be calculated along any azimuth in an image, and α can be

determined as a function of azimuth angle. In this study, the resulting polar plots of azimuth and range were smoothed using a low pass fast Fourier transform filter. Geometric properties were derived from the curves such as orientation, the preferential azimuth, and elongation (Fig 3). Elongation is defined as:

$$\text{elongation} = \frac{\alpha_{\max}}{\perp \alpha_{\max}} \quad (3)$$

the ratio of the maximum range (α_{\max}) and the range perpendicular to the maximum azimuth, $\alpha(\perp \alpha_{\max})$.

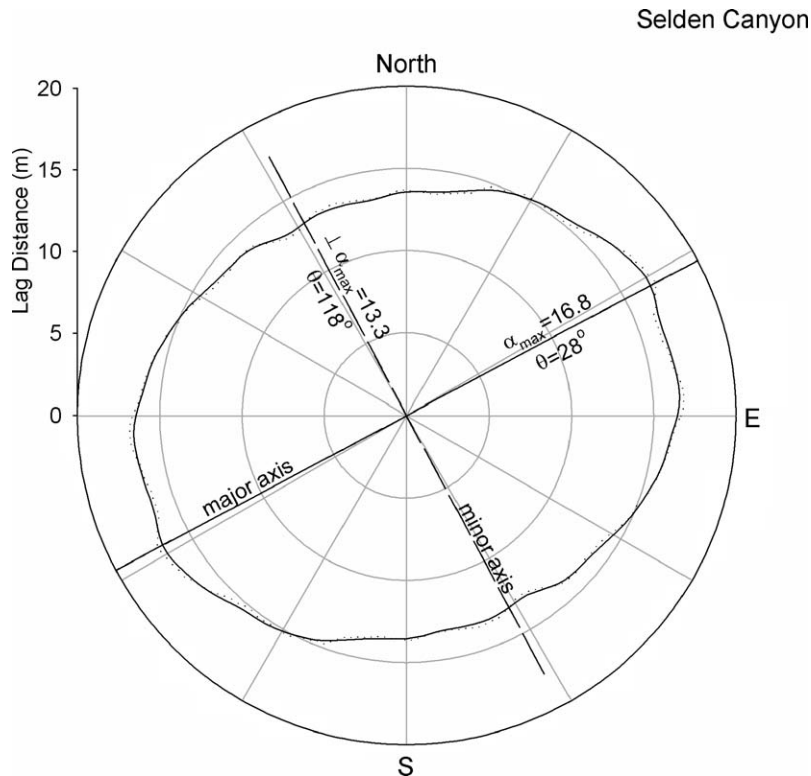


Fig. 3. Polar plot of elongation values (dotted line) smoothed with a Fast-Fourier Transform (FFT) (solid line) and dominant orientation direction from the major axis.

The integration of continuously similar or connected values has been presented in broad applications of geospatial components. Investigations into water transport include spatial connectivity of river channels (Krishnan & Journel, 2003) fractured rocks with three-dimensional percolation from small-to large-scale fault networks (Bour & Davy, 1998), the spatial density of connectivity of fracture networks in rocks with interest in water transport (Renshaw, 1999), and homogenous soil moisture patterns (Western et al., 1998). Incorporation of our connectivity statistic may expand the usage of multiple-point spatial distributions in hydrogeology and throughout the environmental sciences.

2.2. Connectivity simulations

To verify that connectivity provides a robust representation of spatial patterns in remote sensing imagery, a series of tests were performed on simulated images created using the geostatistical software package GSLib (Deutsch & Journel, 1998). The simulated images were generated using the unconditional simulated annealing algorithm with variogram constraints. In one test, normalized anisotropic Gaussian variograms (sill=1, nugget=0) were utilized, with the major axis having a range of 10 and the minor axis having a range of 6. Nineteen sets of 200×200 pixel images were generated using this variogram model with the direction of the major axis varying from 0° to 180° at 10° intervals, with an additional duplicate at 90° (Fig. 4). Three stochastic simulations were produced at each angle interval. This resulted in a total of 57 8-bit images with values between 0 and 99. A 3×3 mean pixel filter was applied to remove individual isolated pixels and fill patches to more accurately mimic the solid clumps observed in natural settings, and a threshold was chosen to convert the image into a binary classification. Connectivity calculations were then performed individually on each of the 57 images.

In a second test, the relation between variogram range and connectivity was explored by the generation of 11 sets of 200×200 pixel isotropic images with range values from 1 to 20 pixels and one set at 40 pixels using the same variogram model (Fig. 5). The simulated images provided a direct analysis of the dependence of connectivity on patch size. A 3×3 mean pixel

filter was then applied to the resulting 33 8-bit images with values between 0 and 99. For each image the cumulative distribution function (CDF) was calculated, allowing the creation of images with a specified fraction of each image below a specific threshold determined from the CDF. These images mimic in appearance orthophotos classified into shrub and not-shrub classes, with the scale of shrub patches defined by the range of the variogram used to in the simulation. Connectivity range calculations were performed on images with simulated cover varying from 10% to 90% in 10% increments. The mean connectivity range of three realizations with each variogram range and fractional cover are reported.

2.3. Study area

The connectivity method provides a quantitative method to measure the vegetation characteristics in different landscapes. Connectivity was tested on a series of images from the Jornada Experimental Range (JER), located in the Chihuahuan Desert of New Mexico, near the town of Las Cruces (Fig. 6). This area has experienced dramatic changes in vegetation cover from semiarid grasslands to arid shrubs. Detailed discussions provided by Buffington and Herbel (1965) and Gibbens et al. (2005) describe the Jornada transition from primarily native perennial grasses (*Bouteloua* spp.) to drought resistant mesquite (*P. glandulosa*) and creosote (*Larrea* spp.). This form of arid land degradation has been attributed to climate change and intensive land use for pastoral purposes.

This study focuses on the distribution of shrubs in the sand sheet area of the Jornada Basin that comprises the western portion of the JER (Fig. 7). The sand sheet exists as a mosaic of patches ranging from mesquite coppice dunes with little to no grass cover to grasslands with isolated mesquites. There are almost no areas in the JER sand sheet that do not contain some mesquite.

2.4. Classification of high-resolution aerial photography

The spatial distribution of vegetation can be ascertained from connectivity calculations of high-resolution aerial photography, which must be first separated into a binary classification of

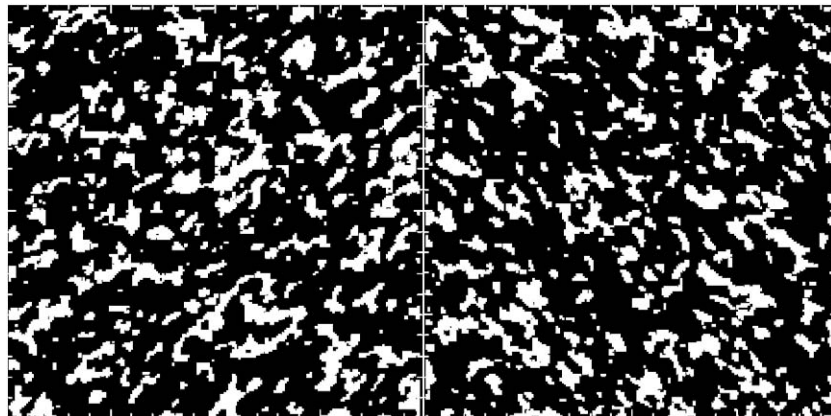


Fig. 4. Simulated images at 40° and 140° orientation with 20% cover used for testing connectivity orientation angle.

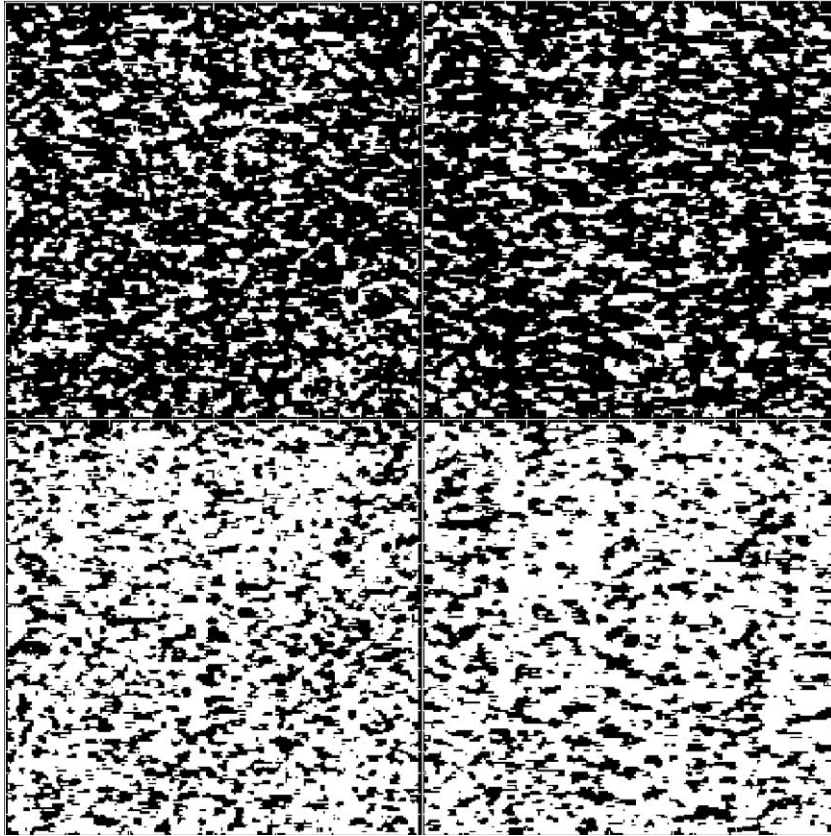


Fig. 5. Simulated images at 0° orientation with 30% (top) and 70% (bottom) cover and a controlled range of 5 (left) and 10 (right) pixels.

interest. Connectivity can only be calculated for images with a binary representation of 1 for the class of interest and 0 for all other classes (Eq. (1)). The use of connectivity is independent of the choice of classification scheme. When shrubs are defined as the class of interest, connectivity calculations provide informa-

tion about the size and shape of shrubs. When the non-shrub classes are defined as the class of interest, connectivity provides information about the size and shape of intershrub patches.

An object-oriented supervised classification was performed on seven digital orthophoto quarter quadrangle (DOQ) natural



Fig. 6. Location of the Jornada Experimental Range (JER) in south central New Mexico.

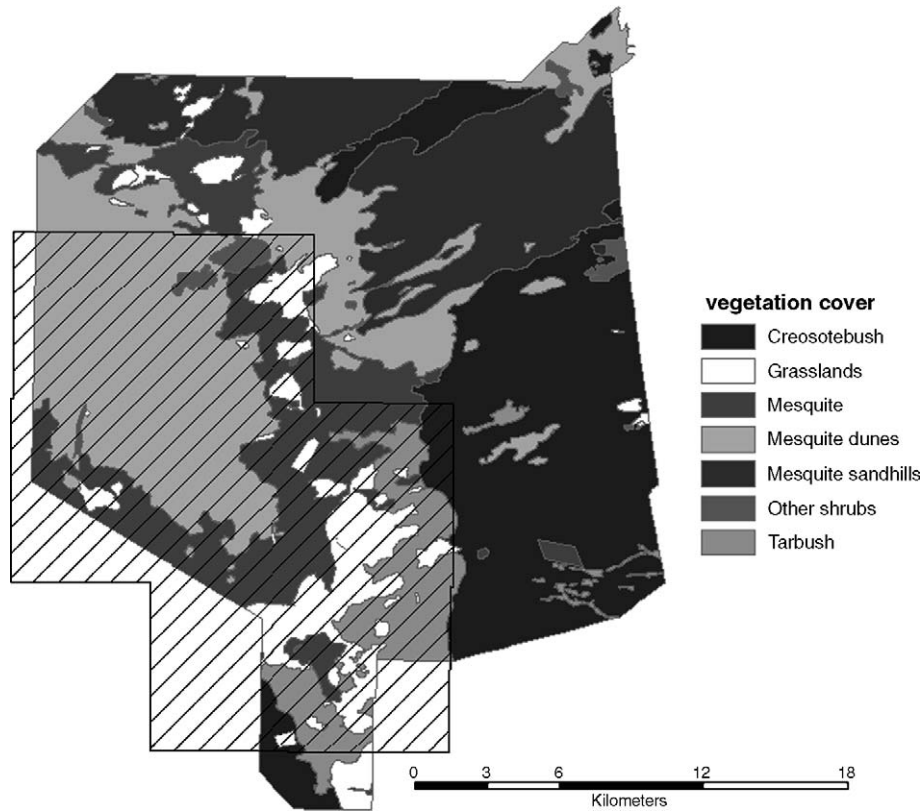


Fig. 7. Aerial coverage of digital orthophotos used in this study from October 1996 (striped) and land cover stratification (modified from Gibbens et al., 2005).

color aerial photos, originally flown by the USGS in October 1996. One-meter ground pixel resolution imagery provides sufficient detail to derive relevant spatial information on mesquite shrubs found in the Jornada sand sheet, as demonstrated by Phinn et al. (1996). Individual mesquite plants larger than 1 m can be identified from the high-resolution imagery and therefore provide an opportunity to examine and extract land cover through both spectral and spatial characteristics through the differentiation of individual shrubs relative to the background of bare soil and grass.

The use of an object-oriented analysis in this study provides many advantages over traditional pixel-based classifications (Geneletti & Gorte, 2003). Object-oriented classification groups adjacent pixels into contiguous multidimensionally homogeneous clusters that represent natural land cover patterns and minimize classification errors that result from single pixels with outlier values and areas of complex spectra due to mixed coverage. Thus, this classification procedure can account for the spatial relationship of pixels, not just the spectral values. This method is gaining increasing acceptance as it proliferates throughout the remote sensing community (Dorren et al., 2003) and has been successfully used by Laliberte et al. (2004) at the JER.

For this study, pixels were identified as shrubs or non-shrub cover through a series of segmentation and classifications in the eCognition software (Fig. 8). The images were divided into object segments according to size, shape and digital number value from all three visible bands. The segmentation process subdivides the images into groups of pixels based on scale-

dependent homogeneity. Single pixels are gradually built-up into larger clusters while accounting for high spectral homogeneity of shrubs relative to soil and the size of shrubs. A maximum object heterogeneity or scale parameter of 6 was used to constrain object sizes and a high emphasis on object compactness and shape to maximize the distinction between shrubs, grasses, and soil. Scale parameter analysis indicated 25% of neighborhoods had a value around 8.62 pixels. All three visible bands had the same spectral weighting for segmentation. Baatz and Schape (2000) provide further description of the segmentation procedure. Supervised classifications were performed on segmented images using a nearest-neighbor approach from the training classes of intensity values for shrub cover, grass cover and soils, and finally grouped according to classes of interest.

While features such as shrubs are easily identified and classified, several limitations are inherent with the use of high spatial-resolution color imagery. Without the availability of high spectral resolution data, it is not possible to accurately distinguish amongst shrub types through a comparison of spectral reflectance. Additionally, centimeter or decimeter-scale vegetation such as grasses cannot be directly detected from meter-scale imagery.

2.5. Connectivity analysis of classified remote sensing imagery

The classified visible digital images were divided into 200×200 pixel subimages in which connectivity was calculated, first with shrubs as the class of interest, then as the non-

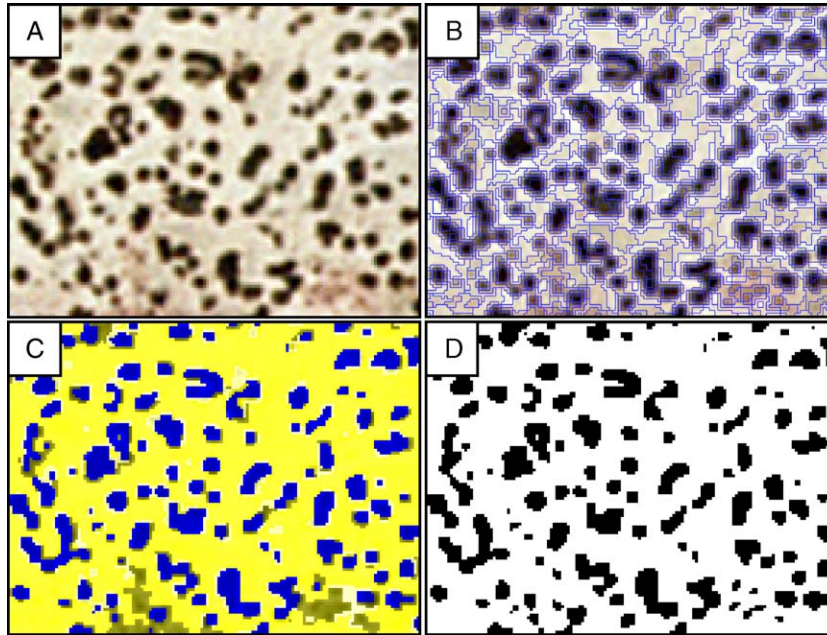


Fig. 8. Object-oriented classification process from (A) digital orthophoto with darker areas represent shrub patches while the lighter background represents grasses and bare soil, (B) image segmentation with irregular shapes representing pixels grouped by shape and similar intensity, (C) supervised classification where segments are grouped into regions of shrub cover (dark), grasses and mixed vegetation (intermediate) and bare soil (light), (D) extracted binary classification feature of shrub (dark) and no-shrub (light).

shrub component as the class of interest. These calculations were performed for lag distances from 0 to 40m, at 2° intervals from 0° to 360° . Range, elongation, and orientation values for each subimage were then integrated into a new coregistered image with 200×200 m pixels. When range, elongation, and orientation are calculated with shrub as the class of interest, these statistics provide information about the size and shape distribution of contiguous areas occupied by shrubs. When these statistics are calculated with the non-shrub class of interest, they provide information about the size and shape distribution of intershrub areas that may be comprised of bare soil, grasses, or a mixture of bare soil and grasses.

2.6. Environmental stratification

The range, geometric elongation, and orientation data were stratified based on a dominant vegetation land cover map, developed from field studies in 1998 (Gibbens et al., 2005). The dominant land cover classification in each subimage was determined and compared with calculated connectivity range, elongation, and orientation. Stratifying orientation and elongation results based on vegetation cover allows for the comparison of shrub distribution within regions of variable shrub infestation.

3. Results

3.1. Connectivity analysis of simulated images

The connectivity method presented here can determine the direction of anisotropy in simulated images. Fig. 9 shows a strong 1:1 relationship between the orientation angle calculated

from connectivity and the major-axis of anisotropy used to generate the simulated images (expected angle). The relationship between the range of isotropic variograms used to generate simulated images and the connectivity range is shown in Fig. 10. The connectivity range increases with increasing variogram range, but flattens out when variogram range reaches about 10 pixels. The connectivity range is also a function of the fractional cover in simulated images, with lower cover resulting in lower connectivity ranges, when connectivity is calculated on the basis of the cover class. When connectivity is calculated on the basis of the non-cover class, lower cover results in greater connectivity ranges (not shown). These results show that connectivity is able to provide an indication of both the direction of anisotropy and an index of the patch size in simulated images. The index of patch size provided by connectivity (e.g., the connectivity range) is different from that provided by the variogram range used to produce the simulated images. This is due to the fact that connectivity provides a fundamentally different measure of spatial autocorrelation than variograms. Thus, connectivity can be used to augment spatial information from traditional variography and can provide important measures of patch size for categorical data.

3.2. Object-oriented classification

The use of 1m orthophotos imagery provides a suitable resolution to detect the presence of shrubs (Laliberte et al., 2004). Due to the size, grass clumps are difficult to distinguish from the soil background, although further study may overcome this limitation to separate shrubs, grass-covered soils, and bare soils at 1m resolution. As a result, classification of the

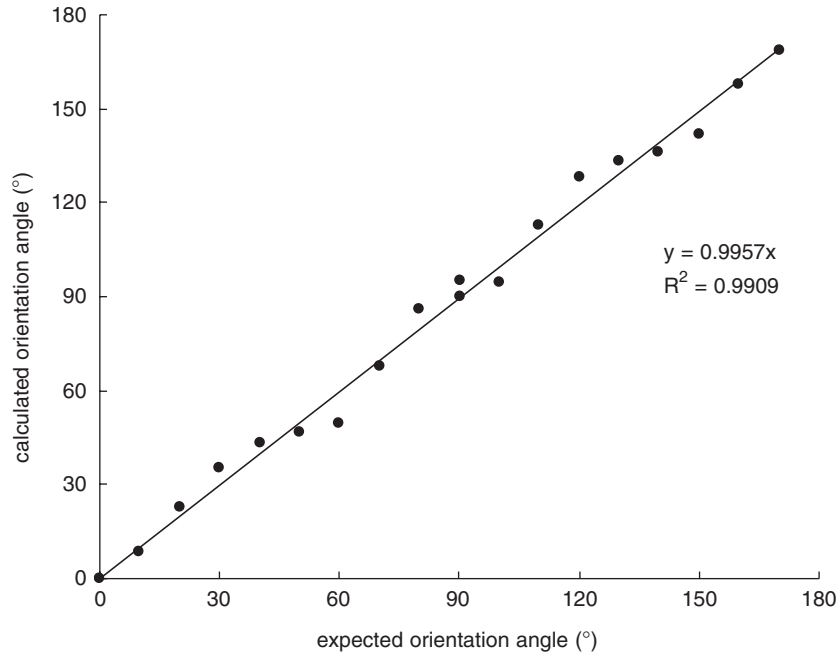


Fig. 9. Calculated orientation angle versus expected orientation angle for images created using the simulated annealing algorithm in GSLIB. Expected orientation angle is the angle of the major-axis of the variogram used to create each image. Calculated orientation angle is the angle of orientation determined by the connectivity method presented here. Each point is the mean for three realizations (generated images) at 20% cover.

orthophotos images with eCognition resulted in maps of the presence or absence of mesquite shrubs, the dominant shrub in the sandsheet are of the JER. Most of the area was classified as bare soil and grasses, while only 14% of pixel area was classified as shrubs (Table 1). Shade dominated pixels may have been misclassified as shrubs in two of the seven images, although unlikely due to visual inspection, spectral differentiation of land cover, the geometric profile of topographically high shrubs, and relatively low leaf area index (LAI) typical of

vegetation in October. The maps of mesquite resulted in estimates of fractional cover consistent with other reports (Laliberte et al., 2004; Okin & Gillette, 2001).

3.3. Shrub connectivity range, elongation, and orientation

Connectivity calculations performed on 200×200m sub-images using the shrub class as the class of interest provide information on the size and shape of shrub patches. Major-axis,

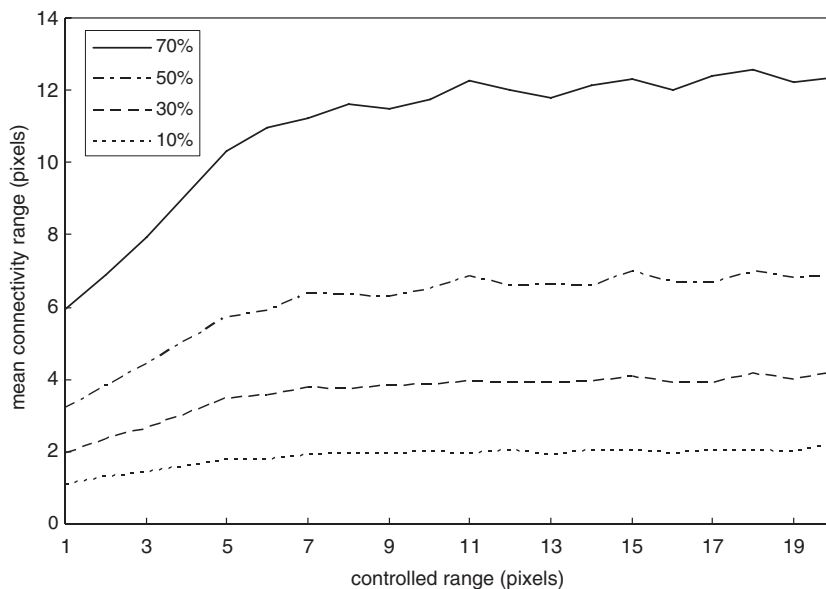


Fig. 10. Calculated range distances versus control range sizes for images created using the simulated annealing algorithm in GSLIB. Controlled range is the size of the x and y axes of the variogram used to create each image. Mean connectivity range is the range distance determined by the connectivity method presented here, calculated at 10%, 30%, 50%, and 70% of image cover. Each point is the mean of the major and minor range values for three realizations.

Table 1
Major-axis range corresponding to dominant vegetation cover

Land cover class	Maximum range (m)		Mean range (m)		Median range (m)		S.D.		% cover
	Shrub	Intershrub	Shrub	Intershrub	Shrub	Intershrub	Shrub	Intershrub	
Grasslands	36.0	327.0	3.5	118.9	2.5	101.3	3.4	83.4	5.2
Mesquite	83.1	325.0	3.1	65.2	2.2	39.7	3.8	69.9	13.4
Mesquite dunes	10.9	227.1	2.5	27.8	2.4	22.8	0.6	20.6	15.0

minor-axis, and mean range values for the shrub class are significantly smaller those for the non-shrub class indicating that mesquite shrubs are generally smaller than the spaces between them (Table 1). Median shrub patch size (i.e., median shrub range) does not vary significantly in size with location or the land cover classification from Gibbens et al. (2005), though the standard deviation of the range is less for mesquite dunes than for either mesquite or grassland areas.

Elongation values are constrained to ≥ 1.0 , thus mean and median elongation values are always >1.0 (Table 2). For analysis of elongation values, the ratio of the standard deviation of elongation to the amount that the median value deviates from one provides an index of the organization of the anisotropy akin to the coefficient of variation:

$$\text{Variability Index (VI)} = \text{Standard Deviation of Elongation} \times (\text{Median of Elongation} - 1) \quad (4)$$

As the VI approaches 1, the anisotropy of shrub or intershrub patches becomes increasingly consistent. Shrub patches tend to be the same size and shape and therefore the VI for the shrub class in all cover types is close to 1.0. Shrub patches in mesquite areas having the highest value $VI=1.3$, which indicates a greater diversity of shrub shapes in these areas.

In subimages dominated by mesquite dunes, the major-axis of anisotropy (the direction of the greatest range value) is oriented roughly northeast–southwest (Fig. 11). For mesquite dune subimages, orientation of shrub patches is clustered between 30° and 59° azimuth and orientation intershrub patches ranges from 0° to 59° . In contrast, no clear preferential orientation of shrub patches was detected for those subimages dominated by grass or mixed grass–shrub vegetation.

3.4. Intershrub connectivity range, elongation, and orientation

Connectivity calculations using the non-shrub classes as the class of interest provide information on the size and shape of intershrub areas. The mean range for intershrub patch size varies significantly with landcover (Table 1). Mean and median

distances are noticeably larger for areas of grasslands when compared to mesquite and mesquite dunes. The range of intershrub patch size (the mean distance between shrubs) decreases from 119m in mixed vegetation to 65m in mesquite, and 28m in mesquite coppice dunes. Median range decreases from 101m in grass-dominated areas to 40m in mesquite-dominated areas to 23m in areas dominated by mesquite dunes. The smaller intershrub distances in mesquite dunes indicate a higher density of shrubs in regions of mesquite and mesquite dunes with respect to areas of grasses. Where shrub size is nearly constant, intershrub distances are inversely related to plant density reflecting an increasing continuum in shrub number density from grasslands to mesquite dunes.

VI (Eq. (4)) calculated from elongation values for intershrub patches in areas dominated by grassland and mesquite all deviate significantly from 1.0 indicating a large diversity in intershrub patch shape in these areas. In mesquite dunelands, $VI=1.3$ indicates a consistent intershrub patch shape in these areas, with a slight elongation of 1.1. Values of $VI>1.3$ for intershrub areas in non-dunelands is consistent with irregular mesquite invasion in these areas and increasingly regular, but anisotropic, mesquite establishment, as mesquite density increases until the $VI=1.2$ in mesquite dunelands.

Orientations of intershrub patches show clear a variation between landcover types, generally similar to the orientation differentiation of the shrub class of interests (Fig. 11). A lack of clear preferential orientation is present in grassland and mesquite regions. The strong orientation found for shrubs in a general SW–NE orientation in mesquite dunes cover is also present for intershrub areas in this landcover type.

4. Discussion

Connectivity calculations performed on high resolution digital images provide information on the size and shape of both shrubs and intershrub patches. Stratified by dominant landcover types, variations in shrub and non-shrub distribution reflect the progressive nature of the transition from grassland to

Table 2
Elongation values for 200m \times 200m subimages from different land cover classes

Land cover class	Mean elongation		Median elongation		S.D.		Variability index	
	Shrub	Intershrub	Shrub	Intershrub	Shrub	Intershrub	Shrub	Intershrub
Grasslands	1.1	2.3	1.1	1.3	0.2	11.5	2.5	46.0
Mesquite	1.1	1.3	1.0	1.1	0.1	2.4	2.7	26.1
Mesquite dunes	1.1	1.1	1.1	1.1	0.1	0.1	1.3	1.2

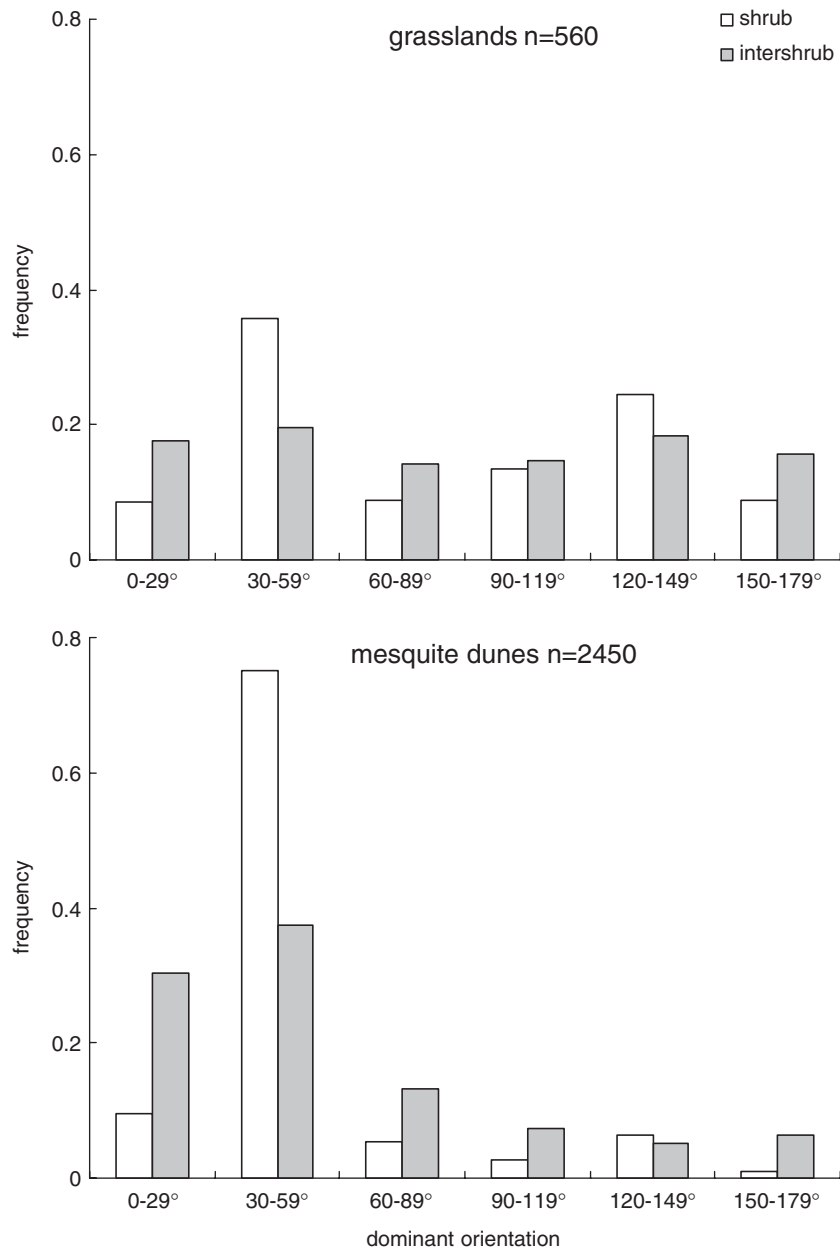


Fig. 11. Histogram of orientation for shrub and intershrub patches for grasslands and mesquite which indicate no preferential orientation, and mesquite dunes showing strong preferential orientation.

shrubland, evident throughout the JER (Gibbens et al., 2005; Laliberte et al., 2004).

Analysis of 1-m orthophotos also provides a direct measurement of the anisotropy of mesquite distribution in the sandsheet portion of the JER. Dominant orientations suggest that the presence of isotropic and anisotropic spatial distribution can be detected using the method presented here. The strength of this anisotropy requires explanation and clearly disputes the widely used assumption of homogeneous (Gillette & Stockton, 1989; Musick and Gillette, 1990) or random (Marticorena & Bergametti, 1995) distributions of land cover in models.

The influences of spatial patterns of vegetation have significant implications for aeolian emission and transport modeling of arid landscape degradation. Shrubs and intershrub

patches in areas of mesquite coppice dunes show a strong northeast–southwest orientation, and agree with earlier studies by Okin and Gillette (2001) and Gillette and Pitchford (2004) that suggested the existence of areas of bare soil with strong windward orientation within regions of mesquite cover called “streets”.

The isotropic orientations found in grasslands indicate a lack of dominant orientation, resulting in a homogeneous or random distribution of mesquite cover. The lack of a dominant orientation in regions of mesquite and amongst grassland vegetation, indicates streets have not developed in these areas. The strong preferential orientation in mesquite dunelands in the Jornada Basin indicates the widespread presence of streets in these areas.

The connectivity results reflect the physical characteristics associated with the respective vegetation cover and must therefore be incorporated within future models of vegetation dynamics and aeolian geomorphology, in addition to providing potential applications beyond aeolian geomorphology. Successful models of landscape dynamics in areas that exhibit strong anisotropy must be able to reproduce these patterns of anisotropy.

Mesquite shrublands dominate, control, and possibly destroy their surrounding environment (Reyes-Reyes et al., 2002; Schlesinger et al., 1990). Connectivity statistics document a marked spatial progression of land cover development. The propagation and development of mesquite shrubs is part of a clear transitional process, influenced by both biotic and abiotic forces, evident in the JER.

Large intershrub distances found in grasslands indicate low shrub density and ideal locations for the establishment of shrubs. Ecological field tests suggest bare soil and to a lesser extent grasslands are regions that allow for root development, soil moisture and nutrient uptake of shrubs with minimal competition from woody vegetation (Schlesinger & Pilmanis, 1998). This initial biotic control is augmented by abiotic factors such as wind erosion, with increased drag and subsequent trapping of water and airborne particles under individual shrubs. Once established, shrubs may cohabitate with grasses and mixed vegetation, but have been observed to be more resilient to environmental and ecological changes, and may therefore allow shrubs to endure even as grasslands are destroyed (Schlesinger et al., 1990; Whitford, 1992).

Relatively constant shrub size across landcover types indicate that mesquite shrubs reach a characteristic size (the range) relatively quickly that generally does not vary over time, even as shrub infestation progresses. Furthermore, since grasslands, mesquite-dominated areas, and mesquite dunelands belong to a continuum of shrub infestation, the results presented here clearly indicate that this process occurs by continual infilling. The process of infilling is distinct from two other conceptions of shrub encroachment: (1) shrub encroachment occurs as an advancing front, and (2) shrub recruitment occurs everywhere in a grassland but the individuals do not increase in size until some threshold is reached when shrubs become dominant and individuals all grow to large size simultaneously. In contrast, infilling is seen as a process where recruitment happens continuously in the landscape and mesquite grow to a large size relatively quickly after successful recruitment.

The progressive development of anisotropic shrub distributions along the grass–mesquite–mesquite duneland continuum strongly indicates that certain sites exhibit higher probability of mesquite establishment than other sites. The correspondence between the major axis of anisotropy in mesquite dunelands and the direction of the prevailing wind at Jornada implicates aeolian transport as a strong control on shrub establishment. Several mechanisms associated with aeolian processes may contribute to the progressive development of anisotropy:

1) Seed dispersal: Although mesquite seeds or seedpods are not particularly prone to dispersal by wind, strong wind events do transport seeds either by creep or saltation. Seeds

transported in this way would tend to be removed from high-energy locations in between shrubs and deposited in low-energy locations under or in the lee of existing vegetation. The distribution of high- and low-energy environments with respect to aeolian transport will be highly oriented in the direction of the prevailing wind direction, resulting in the anisotropic dispersal of seeds.

- 2) Lee-side deposition: The deposition of organic material and fine-grained mineral aggregates in the lee of established mesquite may create suitable microenvironments for the establishment of mesquite by creating areas of high nutrient content and high water holding capacity in these areas.
- 3) Abrasion and scouring in intershrub areas: The high-energy wind environments exhibited in unvegetated areas in between shrubs create streets of high sediment transport (Gillette & Pitchford, 2004). Abrasion of vegetation may increase seedling mortality in these high-energy locations resulting reduced mesquite survival.

The mesquite dunelands in the Jornada sandsheet most likely represent the final stage of the infilling process, due to the highest degree of anisotropy and the highest density of mesquite shrubs. It is unknown at this time whether biotic processes such as competition for water or abiotic processes such as aeolian transport terminate shrub infilling. However, the study of sediment transport in intershrub streets in mesquite dunelands by Gillette and Pitchford (2004) suggests that increased aeolian transport in intershrub areas is a strong candidate.

As the region shifts from homogenous grasslands, shrub encroachment likely disrupts the spatial distribution of nutrients and soil moisture into a heterogeneous clustering in which the distribution of shrubs is influenced by biotic and abiotic processes with varying degrees of anisotropic behavior. This clustering, anchored by the establishment of shrubs creates islands of fertility. Intershrub regions become exceedingly vulnerable to dust emissions and the erosive removal of nutrients and soil moisture.

The loss of exposed topsoil by aeolian processes in intershrub regions inhibits grasslands while encouraging the development of islands of fertility and indicates a major shift from biotic to abiotic influences. Due to the presumed domination of abiotic transport processes within the JER, a strong dichotomy of elongation and orientation would be expected, and is found for shrub cover amongst differing areas of dominant vegetation cover. The detected anisotropy of shrub and intershrub areas that correlates with the prevailing wind direction further indicate the importance of abiotic transport. The dominant preferential orientation detected in areas of mesquite dunes roughly parallels the southwesterly prevailing winds. The absence of a strong preferential orientation in grasslands and moderate orientation in mesquite dominated areas reflects the transitional model for desertification presented by Okin and Gillette (2001) and Schlesinger et al. (1990).

In the progression from homogeneous landscape of grasses to a heterogeneous landscape of shrublands, aeolian processes become increasingly relevant, forcing the moderate orientation of shrubs in the mesquite regions to the highly oriented shrubs in the well-established mesquite dunes region. The increased

propagation of shrubs reduces the connectivity in grasslands. A continuous infilling of shrubs in grasses and mixed vegetation is evident. While the shrubs do not seem to get detectably larger, they force the transition from a biologically controlled region to an aeolian controlled region in which the environment impacts the vegetation and the vegetation impacts the environment. Ultimately, in developed mesquite coppice dunes, shrub cover itself becomes the dominant control on surface geomorphology.

5. Conclusion

The statistical method presented here for calculating landscape connectivity provides a valuable method to quantify spatial connectedness from raster data sets. With appropriate data sets and classification, potential applications extend beyond vegetation dynamics to other areas of the biological and earth sciences, including preserve planning, habitat fragmentation, pore spacing in surface hydrology, microbial community dynamics and other areas where the understanding of the size and arrangement of patches is important.

The primary use of connectivity in this study has been to quantify the spatial distribution of shrubs to provide further insights into process of shrub encroachment in the JER in south-central New Mexico. While complex interaction of multiple biotic and abiotic forces are responsible for shaping the vegetation communities in the JER, the importance of abiotic processes such as aeolian transport become clear in the anisotropy of shrubs and intershrub patches. The spatial distribution and preferential orientation of shrubs in the Jornada Basin that has been demonstrated here provides evidence for infilling as an important component of shrub infestation. Our results also provide a prediction that areas dominated by mesquite in the sandsheet will develop into mesquite coppice dunelands. We anticipate that this will correspond to an increase in aeolian transport and dust emission in these environments.

Woody encroachment is not exclusive to New Mexico and has been observed in areas such as Texas (e.g., Ansley et al., 2001), southern Africa (e.g., Roques et al., 2001), Argentina (e.g., Cabral et al., 2003), and Australia (e.g., Fensham et al., 2005). Integration of connectivity into models of geomorphology and vegetation dynamics in these areas will provide further insight into land degradation processes in arid and semiarid environment, and to achieve comprehensive desertification models.

Acknowledgements

The authors would like to thank Lorelei Hartman for providing helpful comments on drafts of this paper and acknowledge the importance of discussions with Phaedon Kyriakidis in the early stages of this project. This work was supported in part by National Science Foundation grant DEB 03-16320.

References

Ansley, R. J., Ben Wu, X., & Kramp, B. A. (2001). Observation: Long-term increases in mesquite canopy cover in a North Texas savanna. *Journal of Range Management*, 54, 171–176.

- Archer, S. (1995). Tree–grass dynamics in a prosopis-thornscrub savanna parkland—reconstructing the past and predicting the future. *Ecoscience*, 2, 83–99.
- Archer, S., Schimel, D. S., & Holland, E. A. (1995). Mechanisms of shrubland and expansion—land-use, climate or CO₂. *Climate Change*, 29, 91–99.
- Baatz, M., & Schape, A. (2000). Multiresolution segmentation: An optimization for high quality multi-scale image segmentation. In J. Strobl, & T. Blaschke (Eds.), *Angewandte*.
- Bahre, C. J., & Shelton, M. L. (1993). Historic vegetation change, mesquite increases, and climate in southeastern Arizona. *Journal of Biogeography*, 20, 489–504.
- Bour, O., & Davy, P. (1998). On the connectivity of three-dimensional fault networks. *Water Resources Research*, 34, 2611–2622.
- Bradley, B. A., & Mustard, J. F. (2005). Identifying land cover variability distinct from land cover change: Cheatgrass in the Great Basin. *Remote Sensing of Environment*, 94, 204–213.
- Buffington, L. C., & Herbel, C. H. (1965). Vegetational changes on a semidesert grassland range from 1858 to 1963. *Ecological Monographs*, 35, 139–164.
- Cabral, A. C., De Miguel, J. M., Rescia, A. J., Schmitz, M. F., & Pineda, F. D. (2003). Shrub encroachment in Argentinean savannas. *Journal of Vegetation Science*, 14, 145–152.
- Caylor, K. K., Dowty, P. R., Shugart, H. H., & Ringrose, S. (2004). Relationship between small-scale structural variability and simulated vegetation productivity across a regional moisture gradient in southern Africa. *Global Change Biology*, 10, 374–382.
- Deutsch, C. V., & Journel, A. G. (1998). *GSLIB. Geostatistical software library and users guide*, 2nd ed., 3 (p. 69). New York: Oxford University Press.
- Dorren, L. K. A., Maier, B., & Seijmonsbergen, A. C. (2003). Improved Landsat-based forest mapping in steep mountainous terrain using object-based classification. *Forest Ecology and Management*, 183, 31–46.
- Dougill, A. J., & Thomas, A. D. (2004). Kalahari sand soils: Spatial heterogeneity, biological soil crusts and land degradation. *Land Degradation and Development*, 15, 233–242.
- Fensham, R. J., Fairfax, R. J., & Archer, S. R. (2005). Rainfall, land use and woody vegetation cover change in semi-arid Australian savanna. *Journal of Ecology*, 93, 596–606.
- Geneletti, D., & Gorte, B. G. H. (2003). A method for object-oriented land cover classification combining Landsat TM data and aerial photographs. *International Journal of Remote Sensing*, 24, 1273–1286.
- Gibbens, R. P., McNeely, R. P., Havstad, K. M., Beck, R. F., & Nolen, B. (2005). Vegetation changes in the Jornada Basin from 1858 to 1998. *Journal of Arid Environments*, 61, 651–668.
- Gillette, D. A., & Pitchford, A. M. (2004). Sand flux in the northern Chihuahuan Desert, New Mexico, USA, and the influence of mesquite-dominated landscapes. *Journal of Geophysical Research, [Earth Surface]*, 109, F04003, doi: doi:10.1029/2003JF000031.
- Gillette, D. A., & Stockton, P. H. (1989). The effect of nonerodible particles on wind erosion of erodible surfaces. *Journal of Geophysical Research, [Atmospheres]*, 94, 12885–12893.
- Krishnan, S., & Journel, A. G. (2003). Spatial connectivity: From variograms to multiple-point measures. *Mathematical Geology*, 35, 915–925.
- Laliberte, A. S., Rango, A., Havstad, K. M., Paris, J. F., Beck, R. F., McNeely, R., et al. (2004). Object-oriented image analysis for mapping shrub encroachment from 1937 to 2003 in southern New Mexico. *Remote Sensing of Environment*, 93, 198–210.
- Marticorena, B., & Bergametti, G. (1995). Modeling the atmospheric dust cycle: 1. Design of a soil-derived dust emission scheme. *Journal of Geophysical Research, [Atmospheres]*, 100, 16415–16430.
- Musick, H. B., & Gillette, D. A. (1990). Field evaluation of relationships between a vegetation structural parameter and sheltering against wind erosion. *Land Degradation & Rehabilitation*, 2, 87–94.
- Okin, G. S., & Gillette, D. A. (2001). Distribution of vegetation in wind-dominated landscapes: Implications for wind erosion modeling and landscape processes. *Journal of Geophysical Research, [Atmospheres]*, 106, 9673–9683.

- Okin, G. S., & Painter, T. H. (2004). Effect of grain size on remotely sensed spectral reflectance of sandy desert surfaces. *Remote Sensing of Environment*, 89, 272–280.
- Okin, G. S., Roberts, D. A., Murray, B., & Okin, W. J. (2001). Practical limits on hyperspectral vegetation discrimination in arid and semiarid environments. *Remote Sensing of Environment*, 77, 212–225.
- Phinn, S., Franklin, J., Hope, A., Stow, D., & Huenneke, L. (1996). Biomass distribution mapping using airborne digital video imagery and spatial statistics in a semi-arid environment. *Journal of Environmental Management*, 47, 139–164.
- Privette, J. L., Tian, Y., Roberts, G., Scholes, R. J., Wang, Y., Caylor, K. K., et al. (2004). Vegetation structure characteristics and relationships of Kalahari woodlands and savannas. *Global Change Biology*, 10, 281–291.
- Rango, A., Chopping, M., Ritchie, J., Havstad, K., Kustas, W., & Schmugge, T. (2000). Morphological characteristics of shrub coppice dunes in desert grasslands of southern New Mexico derived from scanning LIDAR. *Remote Sensing of Environment*, 74, 26–44.
- Rango, A., Goslee, S., Herrick, J., Chopping, M., Havstad, K., Huenneke, L., et al. (2002). Remote sensing documentation of historic rangeland remediation treatments in southern New Mexico. *Journal of Arid Environments*, 50, 549–572.
- Renshaw, C. E. (1999). Connectivity of joint networks with power law length distributions. *Water Resources Research*, 35, 2661–2670.
- Reyes-Reyes, G., Baron-Ocampo, L., Cuali-Alvarez, I., Frias-Hernandez, J. T., Olalde-Portugal, V., Fregoso, L. V., et al. (2002). C and N dynamics in soil from the central highlands of Mexico as affected by mesquite (*Prosopis* spp.) and huizache (*Acacia tortuosa*): A laboratory investigation. *Applied Soil Ecology*, 19, 27–34.
- Reynolds, J. F., Virginia, R. A., Kemp, P. R., de Soyza, A. G., & Tremmel, D. C. (1999). Impact of drought on desert shrubs: Effects of seasonality and degree of resource island development. *Ecological Monographs*, 69, 69–106.
- Roques, K. G., O'Connor, T. G., & Watkinson, A. R. (2001). Dynamics of shrub encroachment in an African savanna: Relative influences of fire, herbivory, rainfall and density dependence. *Journal of Applied Ecology*, 38, 268–280.
- Scanlon, T. M., Caylor, K. K., Manfreda, S., Levin, S. A., & Rodriguez-Iturbe, I. (2005). Dynamic response of grass cover to rainfall variability: Implications for the function and persistence of savanna ecosystems. *Advances in Water Resources*, 28, 291–302.
- Schlesinger, W. H., & Gramenopoulos, N. (1996). Archival photographs show no climate-induced changes in woody vegetation in the Sudan, 1943–1994. *Global Change Biology*, 2, 137–141.
- Schlesinger, W. H., & Pilmanis, A. M. (1998). Plant–soil interactions in deserts. *Biogeochemistry*, 42, 169–187.
- Schlesinger, W. H., Reynolds, J. F., Cunningham, G. L., Huenneke, L. F., Jarrell, W. M., Virginia, R. A., et al. (1990). Biological feedbacks in global desertification. *Science*, 247, 1043–1048.
- Scholes, R. J., Frost, P. G. H., & Tian, Y. H. (2004). Canopy structure in savannas along a moisture gradient on Kalahari sands. *Global Change Biology*, 10, 292–302.
- Weeks, R. J., Smith, M., Pak, K., Li, W. H., Gillespie, A., & Gustafson, B. (1996). Surface roughness, radar backscatter, and visible and near-infrared reflectance in Death Valley, California. *Journal of Geophysical Research, [Planets]*, 101, 23077–23090.
- Western, A. W., Blöschl, G., & Grayson, R. B. (1998). How well do indicator variograms capture the spatial connectivity of soil moisture? *Hydrological Processes*, 12, 1851–1868.
- Whitford, W. G. (1992). Biogeochemical consequences of desertification. *ACS Symposium Series*, 483, 352–359.